









ORIGINAL ARTICLE

Exercise training alters lipoprotein particles independent of brown adipose tissue metabolic activity

P. Motiani¹ , J. Teuho^{1,2} , T. Saari¹ , K. A. Virtanen^{1,8}, S. M. Honkala¹ , R. J. Middelbeek^{3,4} , L. J. Goodyear³, O. Eskola¹ , J. Andersson⁵, E. Löyttyniemi⁶, J. C. Hannukainen^{1,†}  and P. Nuutila^{1,7,†} 

¹Turku PET Centre, University of Turku, Turku, Finland; ²Department of Medical Physics, Turku University Hospital, Turku, Finland; ³Section on Integrative Physiology and Metabolism, Joslin Diabetes Center, Harvard Medical School, Boston, MA, USA; ⁴Division of Endocrinology, Diabetes and Metabolism, Beth Israel Deaconess Medical Center, Boston, MA, USA; ⁵Section of Radiology, Department of Surgical Sciences, Uppsala University, Uppsala, Sweden; ⁶Department of Biostatistics, University of Turku, Turku, Finland; ⁷Department of Endocrinology, Turku PET Centre, Turku University Hospital, Turku, Finland; ⁸Institute of Public Health and Clinical Nutrition, University of Eastern Finland (UEF), Kuopio, Finland;

Received 17 August 2018; revised 15 January 2019; accepted 17 January 2019

Address for correspondence: Pirjo Nuutila, Turku PET Centre, University of Turku, P.O. Box 52, Turku FIN-20521, Finland. E-mail: pirjo.nuutila@utu.fi

[†]These authors contributed equally for last authorship.

Summary

Introduction

New strategies for weight loss and weight maintenance in humans are needed. Human brown adipose tissue (BAT) can stimulate energy expenditure and may be a potential therapeutic target for obesity and type 2 diabetes. However, whether exercise training is an efficient stimulus to activate and recruit BAT remains to be explored. This study aimed to evaluate whether regular exercise training affects cold-stimulated BAT metabolism and, if so, whether this was associated with changes in plasma metabolites.

Methods

Healthy sedentary men ($n = 11$; aged 31 [SD 7] years; body mass index 23 [0.9] kg m⁻²; VO_{2 max} 39 [7.6] mL min⁻¹ kg⁻¹) participated in a 6-week exercise training intervention. Fasting BAT and neck muscle glucose uptake (GU) were measured using quantitative [¹⁸F]fluorodeoxyglucose positron emission tomography–magnetic resonance imaging three times: (1) before training at room temperature and (2) before and (3) after the training period during cold stimulation. Cervico-thoracic BAT mass was measured using MRI signal fat fraction maps. Plasma metabolites were analysed using nuclear magnetic resonance spectroscopy.

Results

Cold exposure increased supraclavicular BAT GU by threefold ($p < 0.001$), energy expenditure by 59% ($p < 0.001$) and plasma fatty acids ($p < 0.01$). Exercise training had no effect on cold-induced GU in BAT or neck muscles. Training increased aerobic capacity ($p = 0.01$) and decreased visceral fat ($p = 0.02$) and cervico-thoracic BAT mass ($p = 0.003$). Additionally, training decreased very low-density lipoprotein particle size ($p = 0.04$), triglycerides within chylomicrons ($p = 0.04$) and small high-density lipoprotein ($p = 0.04$).

Conclusions

Although exercise training plays an important role for metabolic health, its beneficial effects on whole body metabolism through physiological adaptations seem to be independent of BAT activation in young, sedentary men.

Keywords: Brown adipose tissue, exercise training, glucose uptake, nor-epinephrine, positron emission tomography.

Introduction

Active human brown adipose tissue (BAT) is able to consume lipids and glucose to generate heat by activating mitochondrial uncoupling-protein-1 (1). BAT is inversely

associated with body mass index (BMI), adiposity and outdoor temperature (2–5). BAT transplantation studies in mouse models of obesity have shown decreases in body weight (6). However, there is no direct or indirect evidence suggesting that enhanced BAT metabolism

improves weight management in humans. The role of BAT in human obesity is still uncertain, although several studies support the concept that low level of BAT activity may predispose to obesity (4). It has been estimated that fully activated BAT can contribute up to 5% of basal metabolic rate (7). Therefore, the possibility to increase or maintain sufficient BAT activity could be a potential therapy for obesity and metabolic disease in humans (8).

Cold activates BAT in humans (9,10), but the use of long-term cold exposure to activate BAT remains impractical, fuelling research into new strategies of BAT activation (8). Exercise training has been proposed to activate and recruit human BAT (11,12). Both cold and exercise may mediate BAT activity by increasing catecholamines, leading to lipolysis (13,14). Whereas data on the exercise training-induced activation of BAT in humans are sparse and contradictory, findings from rodent studies suggest that exercise training regulates BAT metabolism (15,16).

In humans, case-control studies indicate lower cold-induced BAT volume and activity in trained individuals compared with sedentary individuals measured by [^{18}F] fluorodeoxyglucose (^{18}F -FDG) positron emission tomography combined with computed tomography (PET/CT) (17,18). Similarly, a pilot study reported incidentally lower BAT activity in trained subjects in comparison with control subjects (19). It has been shown that short-term exercise training decreased BAT insulin-stimulated glucose uptake (GU) in subjects with active BAT prior to intervention (20). Recently, objectively measured physical activity levels were not found to be associated with BAT volume and activity in young healthy sedentary adults (21). Altogether, in humans, exercise appears to be associated with downregulation of BAT glucose metabolism, although further studies are warranted to better understand exercise-induced adaptations of human BAT (17–20). Moreover, regular exercise training reduces body adiposity and improves subject's metabolic profile, but the training effects on the circulating metabolites and BAT metabolism have not been studied simultaneously in a controlled, prospective study.

Previous methods used for BAT analysis in PET/CT and PET/MRI have their intrinsic limitations (9,10,22,23). The tissue contrast and sensitivity for soft tissue imaging are considered better in magnetic resonance imaging (MRI) than in CT imaging. Because brown fat is distributed among white fat, the use of metabolic value for threshold is more specific for BAT activity analysis. In this study, the aim was to investigate the effects of regular exercise training on cold-induced BAT GU and mass using ^{18}F -FDG PET/MRI. In addition, the training-induced changes in lipid profile and plasma metabolites and any

associations to tissue-specific glucose metabolism were analysed. Based on a recent review suggesting that shivering links exercise and cold-induced thermogenesis (14), it was hypothesized that long-term exercise training increases BAT activity after cold exposure.

Materials and methods

Subjects

Healthy, sedentary male subjects ($n = 11$) were enrolled into the study (Clinical Trial NCT03359824), after informed written consent was obtained. The study was conducted in accordance with the Declaration of Helsinki, and the study protocol was approved by the ethics committee of the Hospital District of Southwest Finland, Turku (decision 28/1801/2013 §228). Subjects were recruited through newspaper advertisements. The study was performed at Turku PET Centre, University of Turku and Turku University Hospital (Turku, Finland) between August 2013 and May 2015. Inclusion criteria were age 18–45 years; BMI 20–25 kg m^{-2} , normal glycaemic control verified by oral glucose tolerance test (OGTT); no history of exercise on a regular basis (exercising $<3 \text{ d week}^{-1}$) and $\text{VO}_{2\text{max}} < 40 \text{ mL min}^{-1} \text{ kg}^{-1}$ measured by sub-maximal bicycle ergometer test. Exclusion criteria were chronic diseases, any mental or eating disorder, significant use of alcohol, smoking, use of steroids, narcotics or other substances, prior exposure to radiation, abnormal cardiovascular status, physical disability and contraindications to MRI or any other condition that in the opinion of investigator could create a hazard to the subject safety or endanger the study procedures. All subjects were metabolically healthy. One study subject withdrew from the study during the exercise intervention due to personal reasons.

Study design

At the initial screening visit, a medical history, physical examination, electrocardiography, indirect calorimetry at room temperature, blood sampling and a 2 h 75 g OGTT were performed. This was followed by sub-maximal bicycle ergometer test on another day. Each subject underwent three [^{18}F]FDG PET/MRI scans at overnight fasting conditions. The first scan was performed before exercise training at room temperature, the second scan before exercise training under cold exposure and the third scan after exercise training during cold exposure (Figure 1A). The first and second scans were performed in random order on two separate days, with minimum of 1 week between the two scanning sessions. Once these initial scans were completed, subjects performed 6 weeks

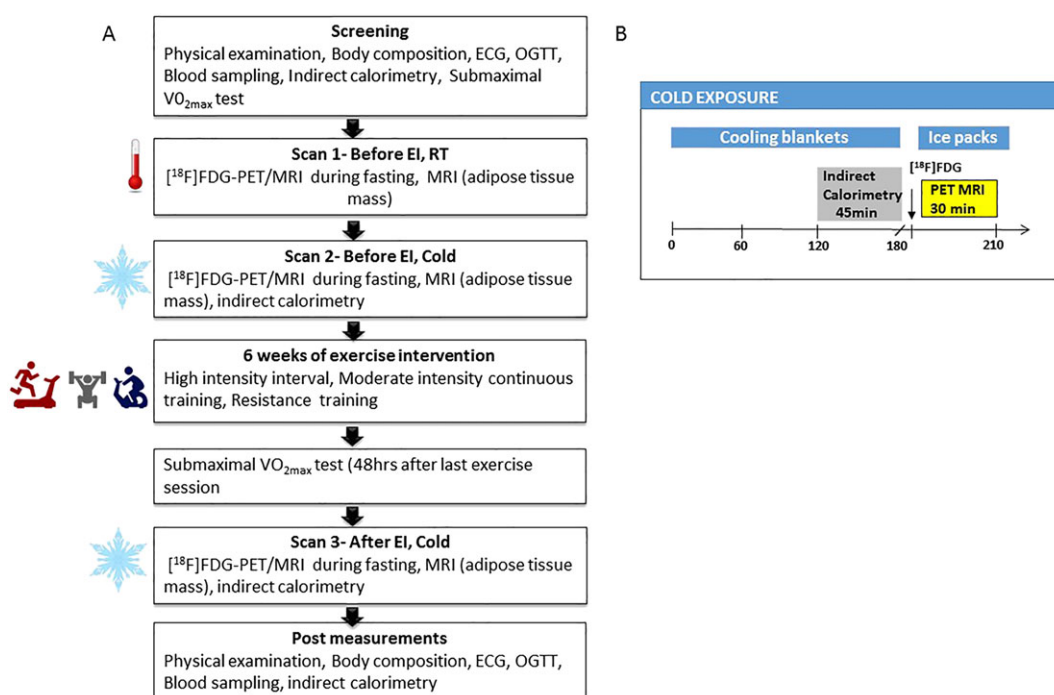


Figure 1 (A) Overview of study design. (B) Protocol of cold exposure

of exercise training (see below). Prior to the third scan, sub-maximal bicycle ergometer was performed 48 h after the last training session. The third PET/MRI scan was performed 48–72 h after the sub-maximal test (except in one subject post 7 d). Indirect calorimetry, OGTT and PET/MRI studies were performed after at least 10 h fast. Caffeinated drinks and alcohol were prohibited ~48 h before the studies. All the screening visit measurements were repeated approximately 48–72 hr after the third PET/MRI scan.

Exercise intervention and bicycle ergometer test

The training intervention was 6 weeks and consisted a combination of moderate-intensity continuous training (MICT, 75–85% of HR_{max}), sprint interval training (SIT, >90% of HR_{max}) and resistance training. MICT included mainly running but also indoor cycling, and cross-trainer exercise was allowed. SIT was performed either by cycle-ergometer (Monark Ergonomic 828E, MONARK, Vansbro, Sweden) or stair-run. Cycle-ergometer SIT training sessions consisted of 5 × 30 s maximal all-out cycling bouts with 4 min recovery between the bouts according to the original protocol by Burgomaster *et al.* (24). Stair-run SIT-training sessions consisted of 6 × 30–45 s maximal stair-run bouts with 4 min recovery between the bouts. The resistance training was divided into two different programmes, leg or upper body-oriented (see details in Table 1). Training loads were individually

determined in the first training session by the participant's ability to complete 10 repetitions for a given exercise. Each week, three of the training sessions were guided by a personal trainer. In addition, beginning in week two of training, subjects performed one to two MICT sessions on their own. All training sessions were monitored via a heart-rate monitor (Suunto, Finland).

The indirect bicycle ergometer test was performed to determine the aerobic capacity of the subjects. The indirect bicycle test was conducted as tripartite sub-maximal test according to the World Health Organization protocol (25). The test started with a 4 min light warm up and was followed by three 4 min work periods with increasing workload. The workloads were determined individually based on the age, BMI and physical activity levels. The cycling frequency was kept at 60 rpm. The cycling intensity was increased so that at the end of the test, the subject reached ~80% of the theoretical maximal heart rate and rating of perceived exertion no more than 17 (Borg scale 6–20). Blood pressure and heart rate were monitored throughout the test. To estimate the VO_{2max} , following formula was used (25):

$$VO_{2max} = \frac{12.35 \times P(w)}{BM(kg)} + 3.5$$

where P = maximal power output based on the workloads and heart rate during the sub-maximal

Table 1 Training protocol

	Mon	Tue	Wed	Thu	Fri	Sat	Sun
Week 1	MICT 30 min		MICT 30 min + resistance training 2		MICT 45 min + resistance training 1		
Week 2	SIT (Wingate-test) + stretching		MICT 30 min + resistance training 2		MICT 45 min + resistance training 1	MICT (independent) 30 min	
Week 3	SIT (Wingate-test) + resistance training 1		MICT 45 min + resistance training 2		SIT (stair-run) + stretching	MICT (independent) 45 min	
Week 4	SIT (Wingate-test) + resistance training 1	MICT (independent) 45 min	MICT 45 min + resistance training 2		SIT (stair-run) + stretching	MICT (independent) 45 min	
Week 5	SIT (Wingate-test) + resistance training 1	MICT (independent) 45 min	MICT 45 min + resistance training 2		SIT (stair-run) + stretching	MICT (independent) 60 min	
Week 6	SIT (Wingate-test) + resistance training 1	MICT (independent) 45 min	MICT 45 min + resistance training 2		SIT (stair-run)	MICT (independent) 60 min	
Resistance training 1 – upper body (Turku PET Centre)							
Resistance training 2 – lower body (Kupittaa sports hall)							
Burpee + Kettlebell swing	3 × 10						
Bicep curl	3 × 10						
Dip push-up	3 × 10						
Push-up	3 × 10						
Plank (max effort)	×3						

Subjects underwent 6 weeks exercise training intervention. Three of the session each week were supervised, and during the weeks 4–6, two sessions were performed individually. SIT, sprint interval training; MICT, moderate-intensity continuous training.

VO_{2max} test, BM = body mass and 3.5 = resting oxygen consumption.

Positron emission tomography–magnetic resonance imaging and magnetic resonance imaging studies

The PET and MRI scans were performed with an integrated 3T Philips Ingenuity TF PET/MR scanner. Both antecubital veins were cannulated for the PET studies; one was used for [^{18}F]-FDG injection and the other one for blood sampling. For the scans performed at room temperature T1 (flip angle 10°, TE 2.3 ms, TR 4.1 ms), weighted MR images and, for cold scans, modified 2-point Dixon images (mDixon, flip angle 10°, TE 1.08 ms, TR 6.5 ms, $\Delta TE = 0.9$ ms) were used to provide anatomical reference. The Dixon cold scans were in total acquired for nine subjects in baseline and for seven subjects after intervention due to technical reasons. For the remainder of cold scans (baseline $n = 2$ and after intervention $n = 3$), T1 weighted MR images were used as anatomical reference.

Personalized cold exposure started 2 h before the PET scan using a cooling blanket (Blanketrol III, Cincinnati Sub-Zero, Cincinnati, OH, USA) (Figure 1B). The cooling was started with 4°C to 6°C water circulating in the cooling blanket. The temperature was gradually raised if shivering was reported by the subjects or visually observed by the investigator. The subjects lay in the supine position under cooling blankets for 2 h, and simultaneously, indirect calorimetry measurements were carried out. After the indirect calorimetry measurements, PET/MRI scanning was performed. During scanning, cooling was maintained by placing iced gel packs on the legs and upper body. Participants remained under cold condition for a total of approximately 3.5 hr from the time of cooling started until the end of the PET/MRI scanning. The skin temperature was measured during scanning using a digital thermometer (Art.183, Termometerfabriken Viking AB, Eskilstuna, Sweden). The temperature sensing probe was attached to the lateral abdominal skin surface. Room temperature (RT) was maintained at ~22°C.

Simultaneously with the injection of [^{18}F]-FDG (Scan 1: 153 [SD 9.0], Scan 2: 155 [SD 7.9], Scan 3: 154 [SD 10.1] MBq) dynamic PET scan was started (frames 7 × 60 s, 4 × 300 s and 1 × 180 s). PET images were reconstructed in a 144 × 144 matrix with an isotropic voxel size of 4 mm, using a fully 3D row action maximum likelihood algorithm (3D-RAMLA) with two iterations and four subsets (26). PET data were corrected for photon attenuation, physical decay, dead time, scatter and random coincidences. Plasma radioactivity was measured with an

automatic gamma counter (Wizard 1480 3", Wallac, Turku, Finland) (27).

Image analysis

Carimas 2.9 software (www.pet.fi/carimas) was used for image analysis. Three-dimensional regions of interest (3D ROIs) were drawn on fused dynamic [^{18}F]-FDG PET and MRI images on supraclavicular BAT, neck white adipose tissue (WAT) and skeletal muscles close to BAT (sternocleidomastoid and levator scapulae) and distant from BAT (deltoid and trapezius muscles). The ROIs were manually outlined from C1 to T4 vertebrae for the muscles within the field of view. Plasma input curves were acquired from PET images by drawing a ROI on the arch of the aorta and corrected from to plasma activity using the haematocrit value. The net influx rate (K_i) was quantified by using graphical analysis of plasma and tissue time-activity curves (Patlak plot) as previously published (10,28). Adipose and muscle regional GU were calculated by multiplying tissue K_i by corresponding plasma glucose concentration and divided by lumped constant. The lumped constant for BAT, WAT and skeletal muscle was set to 1.14, 1.14 and 1.2, respectively (29,30).

BAT mass, in the cervico-upper thoracic region, was estimated from fused cold PET-MRI images before and after exercise intervention using Carimas 2.9 software (www.pet.fi/carimas). MRI signal fat fraction (SFF) maps were created from water component images (W) and fat component images (F) obtained from mDixon sequence using the formula (31).

$$SFF = F / (F + W)$$

The SFF maps were calculated using in-house software developed in MATLAB2015b (Mathworks Inc, Natick, MA) and SPM8 (Wellcome Trust, UCL). A mask was drawn in SFF maps at all potential cervico-upper thoracic BAT sites (cervical, supraclavicular and axillary depots), using a fat fraction threshold of 40% to identify and measure BAT while excluding blood vessels, muscle and bones (19,32,33). The mask was then transferred to the parametric [^{18}F]-FDG PET image to exclude any voxels that had $GU < 3.0 \mu\text{mol}/100 \text{ g min}^{-1}$ GU from the mask. The voxels in the mask then underwent a 2nd thresholding step with $GU > 3.0 \mu\text{mol}/100 \text{ g min}^{-1}$ used to include voxels representing active BAT. Previously, it has been shown that during cold exposure, $GU > 3.0 \mu\text{mol}/100 \text{ g min}^{-1}$ represents active BAT (10). Finally, the volume of all these voxels (cm^3) was converted into mass by assuming the density of BAT to be 0.92 g cm^{-3} (23).

Indirect calorimetry, body composition and nuclear magnetic resonance spectroscopy

The open-system indirect calorimetry (Deltatrac II Datex-Ohmeda) was used for the measurement of O₂ consumption, (VO₂) and CO₂ production (VCO₂). Measurements were performed at RT on screening day and post-training. Data were also collected during the cold exposure before the start of the PET scan, for 45 min both before and after the training intervention. Whole body energy expenditure and substrate utilization were calculated according to the Weir equation (34). For the calculation of protein oxidation rate, urinary nitrogen production was set to be 13 g/24 h. This may result in slight underestimation in carbohydrate utilization and overestimation of lipid oxidation. Body fat content was measured by bioimpedance (Omron BF 400). Abdominal MRI scans were performed to measure abdominal subcutaneous and visceral adipose tissue masses. Fat volumes were analysed using sliceOmatic software v.4.3, and to obtain the tissue mass, the pixel surface area was multiplied by the slice thickness and the density of adipose tissue 0.9196 kg L⁻¹ (35).

Metabolic biomarkers were quantified from plasma of 11 subjects using high-throughput proton NMR metabolomics (Nightingale Health Ltd., Helsinki, Finland). Samples were obtained from the PET scanning day 2 (before exercise training) and day 3 (after exercise training). During both days, the first sample was obtained at RT and the second sample 2 h after the cold exposure from cooling blankets before the administration of ¹⁸F-FDG. Proton NMR spectroscopy provides simultaneous quantification of lipids, lipoprotein subclass profiling with lipid concentrations within 14 subclasses, fatty acid composition and various low-molecular metabolites, including amino acids, ketone bodies and gluconeogenesis-related metabolites in molar concentration units. Details of the NMR metabolomics platform have been previously described (36). Glycerol and glycine were unquantifiable from EDTA plasma sample. Plasma total and high-density lipoprotein (HDL)-cholesterol, triglycerides and glucose concentrations were measured from venous blood samples with an automatized enzymatic assay. Insulin was determined using automatized electro-chemiluminescence immunoassay (Cobas 8000, Roche Diagnostics GmbH, Mannheim, Germany). Low-density lipoprotein (LDL)-cholesterol concentration was calculated using the Friedewald formula. To estimate insulin sensitivity, the Matsuda index was calculated (37). Homeostasis model assessment-estimated insulin resistance was also calculated as previously published (38). We obtained mean daily outdoor temperatures of Turku 2 weeks prior to PET-scanning from (www.sujakapsi.fi).

During the study period, the range of outdoor temperatures was -11.3 to +14.5°C.

Statistics

Results are expressed as model-based means and 95% confidence intervals unless shown otherwise. A paired *t*-test was used to compare mean values of all end points of interest between measurements before and after exercise intervention. Linear mixed models for repeated measurements were used to study mean changes over time. The model included (time; indicating overall mean change between all different time points) and outdoor temperature was taken as a covariate in the model. Compound symmetry covariance structure was used in the analyses. A *p* value of <0.05 was considered statistically significant in all analyses. Pearson correlation was also calculated for the change in variables. Normality was assessed by Shapiro-Wilk test. The variables that did not meet normal distribution were log transformed. All analyses were performed using IBM SPSS software (version 22).

Results

Exercise training improves aerobic capacity and induces changes in plasma lipids and lipoproteins

The 6-week training intervention increased aerobic capacity by +27% and decreased visceral adipose tissue mass by -17% (Table 2). Training decreased plasma triglycerides, total cholines, in particular phosphatidylcholines and fatty acids. Training increased docosahexaenoic acid and citrate concentration (Figure 2A). Training also reduced very low-density lipoprotein (VLDL) particle size, whereas there was no change in LDL and HDL particle size (Figure 3A). Training decreased total lipids and cholesterol within chylomicrons and medium VLDL decreased (Figure 3B,C). Triglycerides decreased within chylomicrons, medium and small VLDL: small LDL and all classes of HDL, except very large and large HDL (Figure 3D).

Cold alters lipoprotein spectrum

Cold increased plasma cholesterol, apolipoproteins, total fatty acids, glutamine, acetate and albumin (Figure 2B), whereas cold had no effect on other metabolites (Figure 4B). Cold also increased the amount of total lipids and total cholesterol in small HDL particles but did not affect particle sizes. (Figure 3E,F,G). After training, cold exposure increased valine and albumin improved lipid metabolism by decreasing apo-lipoprotein B

Table 2 Characteristics of study subjects before and after exercise intervention

	Pre	Post	<i>p</i> -values
Anthropometrics			
Age (years)	31.1 ± 7.5		
BMI (kg m ⁻²)	22.8 ± 1.0	23.1 ± 1.0	0.53
Waist to hip ratio	0.93 ± 0.03	0.91 ± 0.04	0.055
Weight (kg)	73.3 ± 7.7	73.6 ± 8.1	0.51
Fat percentage (%)	17.1 ± 1.7	17.0 ± 1.5	0.20
Fat free mass (kg)	60.6 ± 6.2	61.1 ± 6.4	0.15
Subcutaneous fat mass (kg)	2.2 ± 0.7	2.1 ± 0.4	0.37
Visceral fat mass (kg)	1.1 ± 0.4	0.9 ± 0.4	0.02
VO _{2max} (mL kg ⁻¹ min ⁻¹)	38 ± 9.3	47 ± 8.2	0.01
Glucose profile			
Glucose _{fasting} OGTT day (mmol L ⁻¹)	5.2 ± 0.3	5.3 ± 0.4	0.41
Insulin _{fasting} OGTT day (mmol L ⁻¹)	5.5 ± 2.4	6.1 ± 2.3	0.62
Matsuda index	8.8 ± 4.6	7.4 ± 2.6	0.24
HOMA-IR	1.3 ± 0.6	1.4 ± 0.5	0.58
Lipid profile			
FFA _{fasting} OGTT day (mmol L ⁻¹)	0.39 ± 0.18	0.44 ± 0.19	0.56
Triglycerides _{fP} (mmol L ⁻¹)	0.91 ± 0.30	1.03 ± 0.39	0.23
LDL-cholesterol (mmol L ⁻¹)	2.63 ± 1.14	2.36 ± 0.89	0.18
HDL-cholesterol (mmol L ⁻¹)	1.61 ± 0.32	1.62 ± 0.33	0.97
Total cholesterol (mmol L ⁻¹)	4.7 ± 1.2	4.5 ± 1.1	0.28

Values are means ± SD; *p* values are from paired *t*-tests. fP, fasting plasma; FFA, free fatty acid. Data presented above are from screening day at baseline (pre) and after exercise intervention (post), except visceral and subcutaneous fat mass, which is from scanning days before exercise and after exercise intervention. *p* < 0.05 are marked as bold.

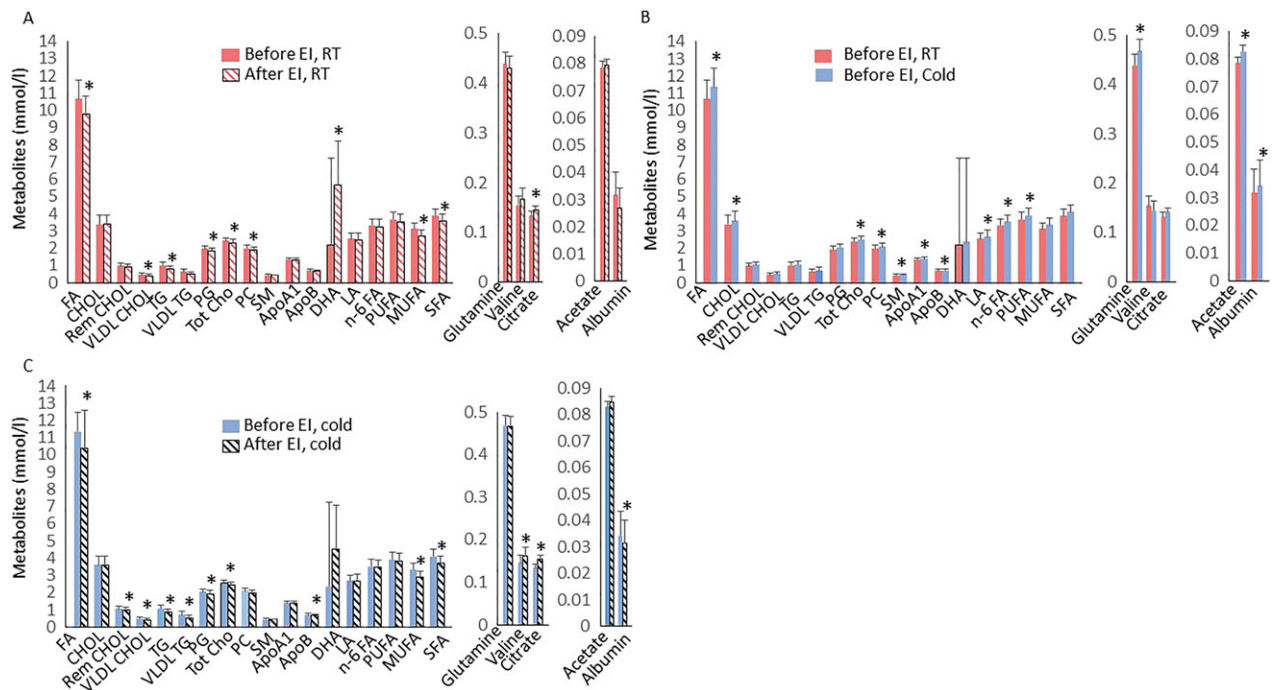
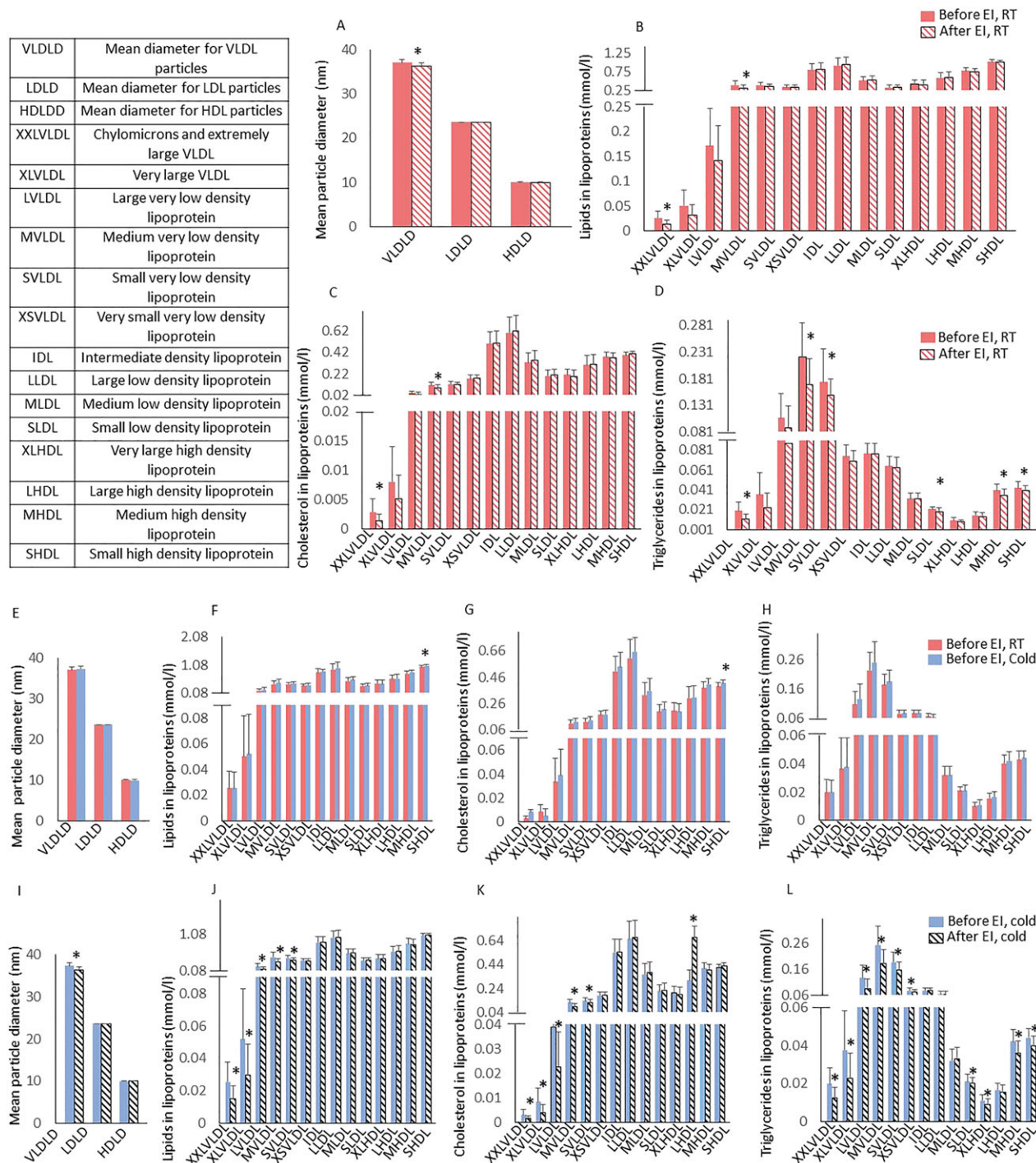


Figure 2 (A) Plasma metabolites at room temperature before exercise intervention (red bars) and after exercise training (patterned red bars), (B) at room temperature (RT) before exercise intervention (red bars) and during cold exposure (blue bars) before exercise intervention, (C) during cold exposure before (blue) and after exercise training (patterned black bars). Values are means ± 95% CI. *p* < 0.05. CHOL, cholesterol; Rem CHOL, remnant cholesterol; VLDL CHOL, very low-density lipoprotein cholesterol; VLDL TG, very low-density lipoprotein triglycerides; PG, phosphoglycerides; Tot Cho, total choline; DHA, decasohexanoic acid; PC, phosphatidylcholines; SM, sphingomyelin; apo A1, apolipoprotein A1; apo B, apolipoprotein B; LA, linoleic acid; n-6 FA, Omega-6 FA; FA, fatty acid; PUFA, polyunsaturated fatty acids; MUFA, monounsaturated fatty acids; SFA, saturated fatty acids



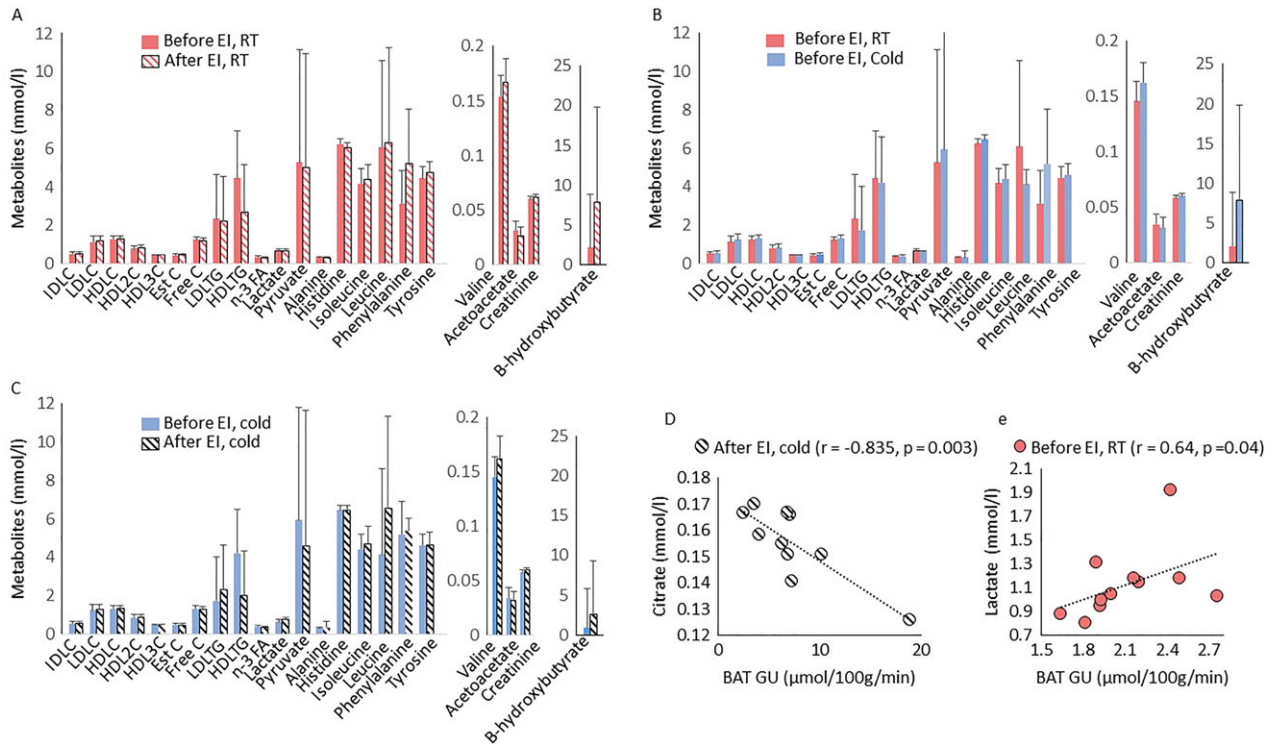


Figure 4 (A) Metabolites at room temperature before (red bars) and after exercise training (patterned red bars), (B) at room temperature (RT) before (red bars) during cold exposure (blue bars) and (C) during cold exposure before (blue) and after exercise training (patterned black bars). (D) Pearson correlation between BAT GU and citrate after exercise intervention at cold. (E) Pearson correlation between BAT GU and lactate at baseline. IDLC; total cholesterol in intermediate density lipoprotein, LDLC; total cholesterol in low density lipoprotein, HDLC; total cholesterol in high density lipoprotein, HDL2C; total cholesterol in high density lipoprotein 2, HDL3C; total cholesterol in high density lipoprotein 3, Est; esterified cholesterol, Free C; free cholesterol, LDLTG, triglycerides in low density lipoprotein, HDL-TG, triglycerides in high density lipoprotein; n-3 FA, Omega-3 fatty acids

(Figure 2C). Among lipoproteins measured during cold, training decreased total lipids and cholesterol within chylomicrons and all classes of VLDL, except very small VLDL and increased cholesterol in large HDL particles (Figure 3J,K). Triglycerides reduced within all sub-classes of VLDL and HDL, except large HDL (Figure 3L).

Effects of cold and training on brown adipose tissue glucose uptake

Cold-exposure increased BAT GU ~3-fold, as compared with RT in all subjects (Figure 5B). In addition, cold increased GU in skeletal muscles located close to BAT +56% (sternocleidomastoid and levator scapulae muscles) but not in muscles distant to BAT (deltoid, trapezius and pectoralis major muscles) and subcutaneous WAT (Figure 5A). When cold-exposure was repeated after 6 weeks of training, no change was observed in cold-induced GU in BAT, WAT or skeletal muscles (Figure 5A). Also, no change was observed in whole body energy expenditure, fat oxidation, and plasma nor-epinephrine and free fatty acid concentrations during cold exposure

after training (Table 3). BAT masses in the cervico-upper thoracic region were highly variable in the study subjects with a mean of 171 ± 31 g (range 135–225 g). Interestingly, cervico-thoracic BAT mass decreased by –42% after training ($p = 0.003$, Figure 5C). At baseline (RT), there was a correlation between BAT GU and plasma lactate (Figure 4E), while during cold, there was a positive association between the cold-stimulated BAT GU and whole body energy expenditure before ($r = 0.86$, $p = 0.006$) and after exercise training ($r = 0.72$, $p = 0.02$). Interestingly, the change in BAT GU correlated inversely with the changes in outdoor temperature (Figure 5D).

Discussion

This study is one of the first clinical intervention trials to investigate BAT metabolism during cold after exercise training. This study design maximized BAT detection by applying gold standard PET-scanning methodology, cold exposure and well-controlled laboratory conditions (39). As expected, exercise training increased aerobic capacity

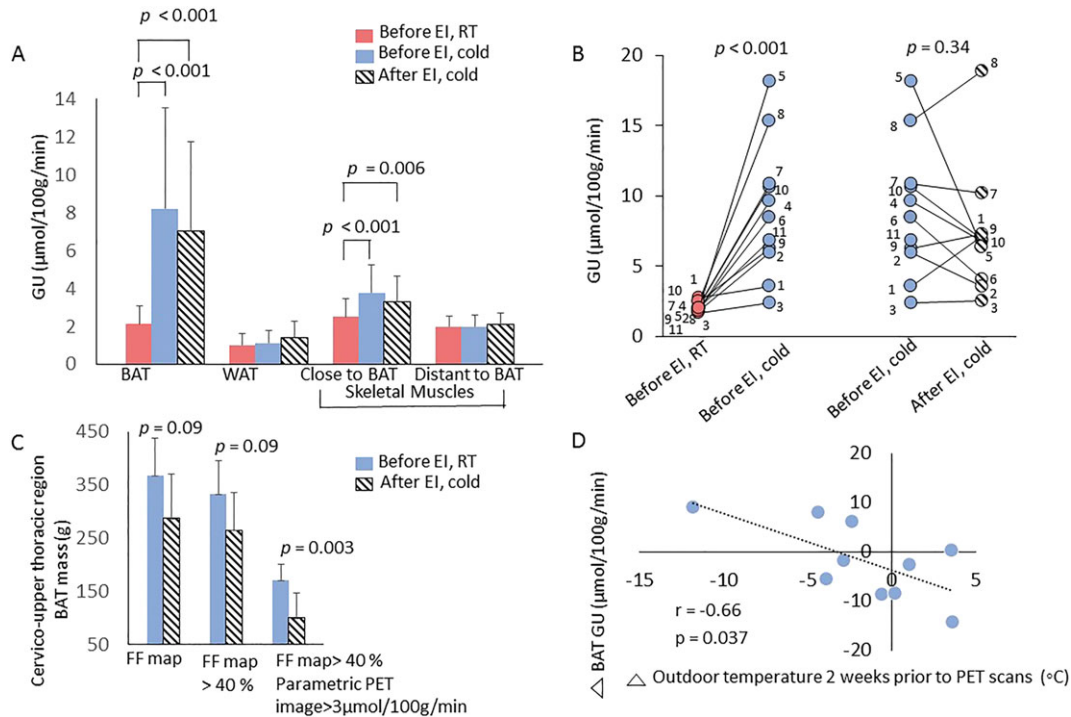


Figure 5 (A) Glucose uptake (GU) was increased during cold both before and after exercise intervention (EI) compared with room temperature (RT) in BAT and less but significantly also in muscles close to BAT area. (B) Individual BAT glucose uptakes during cold exposure were not associated with exercise intervention, but the change in BAT GU correlated inversely with the changes in outdoor temperature (D). (C) (a) BAT mass ($n = 7$) was studied starting with MRI signal fat fraction (SFF) maps of potential cervico-upper thoracic BAT sites. (b) Thresholding >40% cleaned non-adipose structures off. (c) When BAT masses were estimated thereafter by thresholding only areas with concomitant parametric BAT GU > $3 \mu\text{mol}/100 \text{g min}^{-1}$, exercise seems to decrease the mass of BAT. * $p = 0.03$, paired sample Student's t -test \pm SD

and decreased visceral fat mass. Exercise altered the lipoprotein profile, inducing increases in cholesterol within large HDL and decreases in triglycerides within all sub-classes of VLDL and HDL, except large HDL. Interestingly, and contrary to our hypothesis, a 6-week training intervention did not affect cold-stimulated BAT GU but decreased cervico-thoracic BAT mass in healthy sedentary men. These data suggest that training exerts positive effects on whole body metabolism, but these effects seem to occur independently from BAT activation. This study also extends the previous observations showing that changes in BAT GU negatively correlate with changes in outdoor temperature in sedentary adult males.

The main finding of this study is that regular exercise training for 6 weeks did not affect cold-stimulated BAT GU in healthy sedentary men. These findings differ from the results by Vosselman *et al.*, which demonstrated lower cold-stimulated BAT GU in endurance trained athlete compared with lean sedentary subjects in a cross-sectional study design (40). This discrepancy is most likely due to different methods used to quantify BAT GU. Vosselman *et al.* quantified BAT GU based on semi-quantitative standard uptake values (SUV) (40). The drawback of using SUV is that the changes of the

biodistribution of FDG in the body is neglected. For instance, if cooling induces muscle shivering and thereby enhances GU slightly into skeletal muscles, it decreases plasma concentration of FDG and its retention into BAT, which is not taken into account when calculating SUV. In the current study, dynamic PET data were used, and an intervention study for sedentary subjects was conducted. In dynamic imaging, multiple images at different time points are acquired giving a possibility to create a time-activity curve of the rate of ^{18}F -FDG in BAT (41–43). This method allows better assessment of both tracer uptake and retention compared with static imaging in which only one single time frame is selected to reflect overall tracer metabolism (42).

Because lipid utilization increases after exercise training, glucose may not be a primary fuel for BAT after training. However, this hypothesis warrants further investigation. Interestingly, a recent study showed that exercise causes the release of a BAT-derived lipid species 12,13-dihydroxy-9Z-octadecenoic acid (12,13-diHOME) that increases the supply of fatty acids into working muscles, indicating an important role of BAT in regulating the lipid metabolism rather than glucose in response to exercise (44).

Table 3 Energy oxidation and other parameters during thermoneutral condition and cold exposure before and after exercise training intervention

Parameter	Before intervention		After intervention		Before		After	
	RT	Cold	RT	Cold	RT vs. cold	RT vs. cold	RT vs. cold	RT*Time
Mean skin temperature (°C)	33.1 [32.0, 84.2]	32.0 [30.9, 33.1]	33.3 [32.2, 34.4]	33.1 [31.9, 34.2]				
Glucose _{fasting} FDG day (mmol L ⁻¹)	5.4 [5.0, 5.4]	5.3 [5.1, 5.5]	5.4 [5.2, 5.6]	5.3 [5.1, 5.5]	0.008	0.008	0.57	0.69
Insulin _{fasting} FDG day (mmol L ⁻¹)	6.3 [4.9, 7.7]	5.4 [3.9, 6.8]	6.6 [5.1, 8.1]	4.6 [3.1, 6.1]	0.27	0.27	0.03	0.71
FFA _{fasting} FDG day [§] (mU L ⁻¹)	0.45 [0.3, 0.6]	0.56 [0.4, 0.8]	0.43 [0.3, 0.6]	0.58 [0.4, 0.8]	0.21	0.21	0.13	0.69
Whole body EE (Kcal d ⁻¹)	1674 [1425, 1922]	2622 [2352, 2891]	1804 [1549, 2059]	2662 [2400, 2923]	< 0.001	< 0.001	< 0.001	0.85
Whole body EE/FFM (Kcal d ⁻¹)	27.5 [25, 30]	43.0 [40, 46]	29.5 [27, 32]	43.7 [41, 46]	< 0.001	< 0.001	< 0.001	0.25
CHO oxidation (Kcal d ⁻¹)	677 [449, 906]	744 [476, 1011]	843 [604, 1083]	1053 [801, 1306]	0.69	0.69	0.21	0.25
CHO oxidation/FFM (Kcal d ⁻¹)	11.3 [7.7, 14.9]	11.9 [7.7, 16.2]	13.8 [10.0, 17.6]	17.4 [13.5, 21.4]	0.82	0.82	0.20	0.29
Fat oxidation (Kcal d ⁻¹)	685 [404, 965]	1569 [1258, 1880]	650 [369, 930]	1303 [1009, 1598]	< 0.001	< 0.001	0.001	0.35
Fat oxidation/FFM (Kcal d ⁻¹)	11.0 [6.8, 15.2]	25.9 [21.2, 30.6]	10.5 [6.3, 14.8]	21.2 [16.8, 25.6]	< 0.001	< 0.001	0.002	0.84
Norepinephrine (nmol L ⁻¹)	2.55 [1.5, 3.6]	5.52 [4.5, 6.6]	2.62 [1.5, 3.7]	6.59 [5.5, 7.7]	< 0.001	< 0.001	< 0.001	0.87
Epinephrine [§] (nmol L ⁻¹)	0.25 [0.2, 0.3]	0.24 [0.2, 0.3]	0.27 [0.2, 0.4]	0.24 [0.2, 0.3]	0.84	0.84	0.55	0.90
Mean temperature of cooling blanket (°C) 0–60 min		6.9 [5.5, 8.2]		7.1 [5.7, 8.5]				0.75
60–120 min		12.3 [10, 15]		12.0 [10, 14]				0.65

All values are model-based means (95% confidence intervals), FFA, free fatty acids; EE, energy expenditure; FFM, fat free mass; CHO, carbohydrate. The *p*-value for RT*Time interaction indicates significant differences before and after exercise intervention in between the variables measured at room temperature on the scanning days. The *p*-value for Cold*Time interaction indicates significant differences before and after exercise intervention in between the variables measured at cold exposure on the scanning days.

[§]Log transformation was performed to achieve normal distribution. *p* < 0.05 are marked as bold.

In line with previous studies, the present study confirmed that cold exposure increased GU in BAT and skeletal muscles located in the close proximity to BAT but not in muscles distant to BAT (9,10). This could be because cold exposure evoked shivering in skeletal muscles close to BAT. Although the protocol was designed to study BAT under non-shivering conditions, it is inevitable to avoid shivering given the greater mass of skeletal muscles (42%) compared with BAT (1%) of total body weight in adult humans.

Previous studies suggest that outdoor temperature impacts BAT GU (4,5). Saito *et al.* showed an increase in cold-induced BAT GU in healthy volunteers during winter, when compared with summer time (4). It has been suggested that the increased BAT GU may be due to cold-induced BAT hyperplasia (4). Interestingly, there was an inverse correlation between the absolute change in the outdoor temperature (after training scan – baseline scan) and in the absolute change in the cold-stimulated BAT GU before and after the exercise intervention. These results suggest that exposure to higher outdoor temperatures lowers BAT GU especially in subjects scanned in the beginning of summer (May to June). However, outdoor temperature was taken into account in the model and did not confound our results.

There was significant reduction in cervico-thoracic BAT mass estimated using MRI SFF maps. This is in line with rodent data showing a significant decrease in BAT mass after chronic endurance training (45). It has been previously shown that weight loss does not change BAT mass in subjects with obesity but tended to increase BAT GU (46). It is of note that in subjects with morbid obesity, cooling may not be optimal to induce BAT thermogenesis, or subjects with morbid obesity may lack active BAT altogether (47). Interestingly, in the same study, there was no association between 12.5% weight loss and cold-induced BAT GU even though subjects with obesity had high BAT GU values (46). In contrast to another study in subjects with morbid obesity, after 8 months of surgery, body mass reduction of around 28% had a more efficient effect to induce BAT activation in non-diabetic than in subjects with diabetes (48). Surprisingly, in the present study, there was a significant reduction in BAT mass without any changes in body weight or cold-induced BAT GU rate. Moreover, there was a reduction in visceral fat mass, but it did not correlate with reduced cervico-thoracic BAT mass. Based on the finding of reduced BAT mass in the present study, it can be speculated that exercise training might have caused lipolysis to fuel BAT thermogenesis (12). Exercise training may induce rapid mobilization of BAT triglycerides, hence reducing BAT mass.

In line with previous studies, there was an increase in aerobic fitness and decrease in visceral adipose tissue

mass after training (49,50). Exercise improved lipid profile and fatty acids measured by NMR. Lipoproteins are a mixture of heterogeneous lipids composed mainly of cholesterol and triglycerides (51). Disruptions in lipoprotein metabolism may play a role in onset of type 2 diabetes (51). Exercise training reduced VLDL particle size. The increase in VLDL size is typically associated with the reduction in HDL cholesterol concentration, in part related to the transfer of cholesterol ester from triglyceride rich lipoproteins to HDL. In addition, when these triglyceride-rich VLDL particles undergo further lipolysis, they give rise to LDL cholesterol. The effects of exercise training on the reduction in medium VLDL were not explained by BAT but rather seems to be the effect of training in general.

Metabolites were measured during cold exposure after exercise with most prominent changes seen within the triglycerides stored in lipoproteins. It has been documented that degradation of triglycerides within VLDL increases during moderate intensity exercise (52). The decrease of mainly VLDL (consisting of lipids, cholesterol and triglycerides) suggests that VLDL provides lipid substrates to help to meet the excess energy demands after exercise. The most pronounced increase in lipoprotein particles was seen in the total cholesterol in large HDL. Large HDL is associated inversely with cardiovascular risk (53). The increase in total cholesterol within large HDL has also been shown in previous training studies (54). Large HDL particles carry cholesterol to the liver for excretion. In the present study, after training, cold exposure had a greater effect in decreasing triglycerides within lipoproteins compared with pre-training situation. This finding suggests that exercise training may reverse the effect of cold to substantially reduce triglycerides. Further work is required to determine the role of cold and exercise training in the regulation of lipoproteins and BAT metabolism. The present data, however, did not validate a direct relationship between BAT GU and changes seen in lipoprotein profile.

Limitations of this study include the relatively small sample size, resulting in reduced statistical power to detect associations. Due to the radiation burden of PET-scanning, it was not possible to repeat RT scanning after training intervention. The aim of personalized cooling protocol was to induce maximal non-shivering thermogenesis in all subjects; however, the method used for the assessment of shivering was subjective. There is a possibility that the present cooling protocol may deliver cold stress of variable degree in different subjects, which may create a bias in cooling response of each subject. The skin temperature was measured only from single specific site (lateral abdominal skin surface) was limitation in terms of thermogenic accuracy. In future studies, detection of muscle shivering by using electromyography and

more detailed measurements of core and skin temperature could be used to ensure the appropriate stimulation of BAT thermogenesis. Only healthy, sedentary men were studied in the current study, which warrants a future prospect of studies in women and subjects with metabolic disorders. In conclusion, exercise training did not affect cold-stimulated BAT GU but decreased cervico-thoracic BAT mass in humans. Exercise-induced changes in lipid particles and metabolites may mediate some of the beneficial effects of exercise on whole body metabolism and may have therapeutic potential for obesity and metabolic diseases independent of BAT activation.

Acknowledgements

We thank all the volunteers who participated in this study, the study nurse Mia Koutu and the staff of the Turku PET Centre and the Paavo Nurmi Centre for their excellent assistance in the study.

Funding

This study was conducted within the Finnish Centre of Excellence in Cardiovascular and Metabolic Diseases supported by the Academy of Finland, University of Turku, Turku University Hospital and Åbo Akademi University. The study was supported by the Academy of Finland (grant numbers 307402 [to P. N.] and 292839 and 269977 [to K. A. V.]), the Paavo Nurmi Foundation, the Finnish Cultural Foundation and National Institutes of Health grant numbers R01-DK099511 and R01-DK112283 (to L. J. G.) and K23-DK114550 (to R. J. W. M.) and P30-DK36836 (Joslin Diabetes Center, Diabetes Research Center, DRC core).

Conflict of interest

The authors declare that there is no duality of interest associated with this manuscript.

Author contributions

P. M. contributed to analysis, result interpretation and to the writing of the manuscript. J. T., J. C. H. and K. A. V. contributed to the acquisition of data. P. N., K. A. V., J. C. H., L. J. G. and R. J. M. contributed to the study design and critical revision of the manuscript for important intellectual content. J. T., S. M. H., T. S., E. L., J. A. and O. E. contributed to data analysis and writing of manuscript. P. N. and J. C. H. contributed to the study design, writing and drafting the manuscript. All authors approved the last version of the manuscript. P. N. is the guarantor of this work and, as such, had access to all study data and takes responsibility for the integrity of the data and the data analysis.

References

1. Cannon B, Nedergaard J. Brown adipose tissue: function and physiological significance. *Physiol Rev* 2004; **84**: 277–359. <https://doi.org/10.1152/physrev.00015.2003>.
2. van Marken Lichtenbelt WD, Vanhommel JW, Smulders NM, et al. Cold-activated brown adipose tissue in healthy men. *N Engl J Med* 2009; **360**: 1500–1508. <https://doi.org/10.1056/NEJMoa0808718>.
3. Cypess AM, Lehman S, Williams G, et al. Identification and importance of brown adipose tissue in adult humans. *N Engl J Med* 2009; **360**: 1509–1517. <https://doi.org/10.1056/NEJMoa0810780>.
4. Saito M, Okamatsu-Ogura Y, Matsushita M, et al. High incidence of metabolically active brown adipose tissue in healthy adult humans: effects of cold exposure and adiposity. *Diabetes* 2009; **58**: 1526–1531. <https://doi.org/10.2337/db09-0530>.
5. Cohade C, Mourtzikos KA, Wahl RL. “USA-Fat”: prevalence is related to ambient outdoor temperature-evaluation with 18F-FDG PET/CT. *J Nucl Med* 2003; **44**: 1267–1270. <http://www.ncbi.nlm.nih.gov/pubmed/12902417>. Accessed June 6, 2018.
6. Soler-Vázquez MC, Mera P, Zagmutt S, Serra D, Herrero L. New approaches targeting brown adipose tissue transplantation as a therapy in obesity. *Biochem Pharmacol* 2018; **155**: 346–355. <https://doi.org/10.1016/j.bcp.2018.07.022>.
7. van Marken Lichtenbelt WD, Schrauwen P. Implications of nonshivering thermogenesis for energy balance regulation in humans. *Am J Physiol Regul Integr Comp Physiol* 2011; **301**: 285.
8. Loh RKC, Kingwell BA, Carey AL. Human brown adipose tissue as a target for obesity management; beyond cold-induced thermogenesis. *Obes Rev* 2017; **18**: 1227–1242. <https://doi.org/10.1111/obr.12584>.
9. Virtanen KA, Lidell ME, Orava J, et al. Functional brown adipose tissue in healthy adults. *N Engl J Med* 2009; **360**: 1518–1525. <https://doi.org/10.1056/NEJMoa0808949>.
10. Orava J, Nuutila P, Lidell ME, et al. Different metabolic responses of human brown adipose tissue to activation by cold and insulin. *Cell Metab* 2011; **14**: 272–279. <https://doi.org/10.1016/j.cmet.2011.06.012>.
11. Ruiz JR, Martinez-Tellez B, Sanchez-Delgado G, Aguilera CM, Gil A. Regulation of energy balance by brown adipose tissue: at least three potential roles for physical activity. *Br J Sports Med* 2015; **49**: 972–973. <https://doi.org/10.1136/bjsports-2014-094537>.
12. Sanchez-Delgado G, Martinez-Tellez B, Olza J, Aguilera CM, Gil A, Ruiz JR. Role of exercise in the activation of brown adipose tissue. *Ann Nutr Metab* 2015; **67**: 21–32. <https://doi.org/10.1159/000437173>.
13. Kolditz C-I, Langin D. Adipose tissue lipolysis. *Curr Opin Clin Nutr Metab Care* 2010; **13**: 377–381. <https://doi.org/10.1097/MCO.0b013e32833bed6a>.
14. Virtanen KA. BAT thermogenesis: linking shivering to exercise. *Cell Metab* 2014; **19**: 352–354. <https://doi.org/10.1016/j.cmet.2014.02.013>.
15. De Matteis R, Lucertini F, Guescini M, et al. Exercise as a new physiological stimulus for brown adipose tissue activity. *Nutr Metab Cardiovasc Dis* 2013; **23**: 582–590. <https://doi.org/10.1016/j.numecd.2012.01.013>.
16. Lehnig AC, Stanford KI. Exercise-induced adaptations to white and brown adipose tissue. *J Exp Biol* 2018; **221**: jeb161570. <https://doi.org/10.1242/jeb.161570>.
17. Vosselman MJ, Hoeks J, Brans B, et al. Low brown adipose tissue activity in endurance trained compared to lean sedentary men. *Int J*

- Obes (Lond)* 2015;(January). doi:<https://doi.org/10.1038/ijo.2015.130>; **39**: 1696–1702.
18. Singhal V, Maffaioli GD, Ackerman KE, et al. Effect of chronic athletic activity on brown fat in young women. *Handelsman DJ, ed. PLoS One* 2016; **11**: e0156353. <https://doi.org/10.1371/journal.pone.0156353>.
 19. Trexler ET, McCallister D, Smith-Ryan AE, Branca RT. Incidental finding of low brown adipose tissue activity in endurance-trained individuals: methodological considerations for positron emission tomography. *J Nat Sci* 2017; **3** <http://www.ncbi.nlm.nih.gov/pubmed/28580427>. Accessed June 6, 2018.
 20. Motiani P, Virtanen KA, Motiani KK, et al. Decreased insulin-stimulated brown adipose tissue glucose uptake after short-term exercise training in healthy middle-aged men. *Diabetes Obes Metab* 2017; **19**: 1379–1388. <https://doi.org/10.1111/dom.12947>.
 21. Acosta FM, Martinez-Tellez B, Sanchez-Delgado G, et al. Association of objectively measured physical activity with brown adipose tissue volume and activity in young adults. *J Clin Endocrinol Metab* August 2018 <https://doi.org/10.1210/jc.2018-01312>.
 22. Muzik O, Mangner TJ, Granneman JG. Assessment of oxidative metabolism in brown fat using PET imaging. *Front Endocrinol (Lausanne)* 2012; **3**: 15. <https://doi.org/10.3389/fendo.2012.00015>.
 23. Din MU, Raiko J, Saari T, et al. Human brown adipose tissue ([¹⁵O]O₂ PET imaging in the presence and absence of cold stimulus. *Eur J Nucl Med Mol Imaging* 2016; **43**: 1878–1886. <https://doi.org/10.1007/s00259-016-3364-y>.
 24. Burgomaster KA, Hughes SC, Heigenhauser GJF, Bradwell SN, Gibala MJ. Six sessions of sprint interval training increases muscle oxidative potential and cycle endurance capacity in humans. *J Appl Physiol (Bethesda, Md 1985)* 2005; **98**: 1985–1990. <https://doi.org/10.1152/jappphysiol.01095.2004>.
 25. Coleman DC. *Fundamentals of Exercise Testing*. World Health Organization: Geneva, pp. 69–76.
 26. Browne J, de Pierro AB. A row-action alternative to the EM algorithm for maximizing likelihood in emission tomography. *IEEE Trans Med Imaging* 1996; **15**: 687–699. <https://doi.org/10.1109/42.538946>.
 27. Tarantola G, Zito F, Gerundini P. PET instrumentation and reconstruction algorithms in whole-body applications. *J Nucl Med Off Publ Soc Nucl Med* 2003; **44**: 756–769.
 28. Gjedde A. Calculation of cerebral glucose phosphorylation from brain uptake of glucose analogs in vivo: a re-examination. *Brain Res* 1982; **257**: 237–274.
 29. Virtanen KA, Peltoniemi P, Marjamäki P, et al. Human adipose tissue glucose uptake determined using [¹⁸F]-fluoro-deoxy-glucose ([¹⁸F]FDG) and PET in combination with microdialysis. *Diabetologia* 2001; **44**: 2171–2179. <https://doi.org/10.1007/s001250100026>.
 30. Peltoniemi P, Lönnroth P, Laine H, et al. Lumped constant for [¹⁸F] fluorodeoxyglucose in skeletal muscles of obese and nonobese humans. *Am J Physiol Metab* 2000; **279**: E1122–E1130. <https://doi.org/10.1152/ajpendo.2000.279.5.E1122>.
 31. Franz D, Karampinos DC, Rummeny EJ, et al. Discrimination between brown and white adipose tissue using a 2-point Dixon water-fat separation method in simultaneous PET/MRI. *J Nucl Med* 2015; **56**: 1742–1747. <https://doi.org/10.2967/jnumed.115.160770>.
 32. Lundström E, Strand R, Johansson L, Bergsten P, Ahlström H, Kullberg J. Magnetic resonance imaging cooling-reheating protocol indicates decreased fat fraction via lipid consumption in suspected brown adipose tissue. *PLoS One* 2015; **10**: e0126705. <https://doi.org/10.1371/journal.pone.0126705>.
 33. Holstila M, Pesola M, Saari T, et al. MR signal-fat-fraction analysis and T2* weighted imaging measure BAT reliably on humans without cold exposure. *Metabolism* 2017; **70**: 23–30. <https://doi.org/10.1016/j.metabol.2017.02.001>.
 34. Weir JBD. New methods for calculating metabolic rate with special reference to protein metabolism. *J Physiol* 1949; **109**: 1–9.
 35. Abate N, Burns D, Peshock RM, Garg A, Grundy SM. Estimation of adipose tissue mass by magnetic resonance imaging: validation against dissection in human cadavers. *J Lipid Res* 1994; **35**: 1490–1496.
 36. Soininen P, Kangas AJ, Würtz P, Suna T, Ala-Korpela M. Quantitative serum nuclear magnetic resonance metabolomics in cardiovascular epidemiology and genetics. *Circ Cardiovasc Genet* 2015; **8**: 192–206. <https://doi.org/10.1161/CIRCGENETICS.114.000216>.
 37. Matsuda M, DeFronzo RA. Insulin sensitivity indices obtained from oral glucose tolerance testing: comparison with the euglycemic insulin clamp. *Diabetes Care* 1999; **22**: 1462–1470.
 38. Matthews DR, Hosker JP, Rudenski AS, Naylor BA, Treacher DF, Turner RC. Homeostasis model assessment: insulin resistance and beta-cell function from fasting plasma glucose and insulin concentrations in man. *Diabetologia* 1985; **28**: 412–419. <http://www.ncbi.nlm.nih.gov/pubmed/3899825>. Accessed June 6, 2018.
 39. Chondronikola M, Beeman SC, Wahl RL. Non-invasive methods for the assessment of brown adipose tissue in humans. *J Physiol* 2018; **596**: 363–378. <https://doi.org/10.1113/JP274255>.
 40. Vosselman MJ, Hoeks J, Brans B, et al. Low brown adipose tissue activity in endurance-trained compared with lean sedentary men. *Int J Obes (Lond)* 2015; **39**: 1696–1702. <https://doi.org/10.1038/ijo.2015.130>.
 41. Chen KYY, Cypess AMM, Laughlin MRR, et al. Brown adipose reporting criteria in imaging studies (BARCIST 1.0): recommendations for standardized FDG-PET/CT experiments in humans. *Cell Metab* 2016; **24**: 210–222. <https://doi.org/10.1016/j.cmet.2016.07.014>.
 42. Muzi M, O'Sullivan F, Mankoff DA, et al. Quantitative assessment of dynamic PET imaging data in cancer imaging. *Magn Reson Imaging* 2012; **30**: 1203–1215. <https://doi.org/10.1016/j.mri.2012.05.008>.
 43. Ong FJ, Ahmed BA, Oreskovich SM, et al. Recent advances in the detection of brown adipose tissue in adult humans: a review. *Clin Sci* 2018; **132**: 1039–1054. <https://doi.org/10.1042/CS20170276>.
 44. Stanford KI, Lynes MD, Takahashi H, et al. 12,13-diHOME: an exercise-induced lipokine that increases skeletal muscle fatty acid uptake. *Cell Metab* 2018; **27**: 1120.e3. <https://doi.org/10.1016/j.cmet.2018.03.020>.
 45. Wu MV, Bikopoulos G, Hung S, Ceddia RB. Thermogenic capacity is antagonistically regulated in classical brown and white subcutaneous fat depots by high fat diet and endurance training in rats: impact on whole-body energy expenditure. *J Biol Chem* 2014; **289**: 34129–34140. <https://doi.org/10.1074/jbc.M114.591008>.
 46. Orava J, Nuutila P, Nojonen T, et al. Blunted metabolic responses to cold and insulin stimulation in brown adipose tissue of obese humans. *Obesity* 2013; **21**: 2279–2287. <https://doi.org/10.1002/oby.20456>.
 47. Vijgen GHEJ, Bouvy ND, Teule GJJ, Brans B, Schrauwen P, van Marken Lichtenbelt WD. Brown adipose tissue in morbidly obese subjects. Fadini GP, ed. *PLoS One* 2011; **6**: e17247. <https://doi.org/10.1371/journal.pone.0017247>.

48. Rodovalho S, Rachid B, De-Lima-Junior JC, et al. Impairment of body mass reduction-associated activation of brown/beige adipose tissue in patients with type 2 diabetes mellitus. *Int J Obes (Lond)* 2017; **41**: 1662–1668. <https://doi.org/10.1038/ijo.2017.152>.
49. Keller C, Steensberg A, Pilegaard H, et al. Transcriptional activation of the IL-6 gene in human contracting skeletal muscle: influence of muscle glycogen content. *FASEB J Off Publ Fed Am Soc Exp Biol* 2001; **15**: 2748–2750. <https://doi.org/10.1096/fj.01-0507fje>.
50. Ghahramanloo E, Midgley AW, Bentley DJ. The effect of concurrent training on blood lipid profile and anthropometrical characteristics of previously untrained men. *J Phys Act Health* 2009; **6**: 760–766.
51. Badeau RM, Honka M-J, Lautamäki R, et al. Systemic metabolic markers and myocardial glucose uptake in type 2 diabetic and coronary artery disease patients treated for 16 weeks with rosiglitazone, a PPAR γ agonist. *Ann Med* 2014; **46**: 18–23. <https://doi.org/10.3109/07853890.2013.853369>.
52. Morio B, Holmbäck U, Gore D, Wolfe RR. Increased VLDL-TAG turnover during and after acute moderate-intensity exercise. *Med Sci Sports Exerc* 2004; **36**: 801–806.
53. Kontush A. HDL particle number and size as predictors of cardiovascular disease. *Front Pharmacol* 2015; **6**: 218. <https://doi.org/10.3389/fphar.2015.00218>.
54. Kodama S, Tanaka S, Saito K, et al. Effect of aerobic exercise training on serum levels of high-density lipoprotein cholesterol: a meta-analysis. *Arch Intern Med* 2007; **167**: 999–1008. <https://doi.org/10.1001/archinte.167.10.999>.